Applied Catalysis B: Environmental 259 (2019) 118030

Contents lists available at ScienceDirect

Applied Catalysis B: Environmental

journal homepage: www.elsevier.com/locate/apcatb

Degradation of *p*-nitrophenol using a ferrous-tripolyphosphate complex in the presence of oxygen: The key role of superoxide radicals

Chengwu Zhang, Tianyi Li, Jingyi Zhang, Song Yan, Chuanyu Qin*

Key Laboratory of Groundwater Resources and Environment, Ministry of Education, Jilin University, Changchun 130021, China

ARTICLE INFO

Keywords:
p-Nitrophenol
Ferrous–polyphosphate/O_2system
Oxygen activation
Superoxide radical

ABSTRACT

It has been recognized that a ferrous–polyphosphate complex can activate oxygen to produce reactive oxygen species (ROS) capable of degrading organic compounds. ˙OH has been confirmed as the predominant ROS. However, the role of $O_2^{\bullet-}$ during the degradation of these contaminants has not been clearly explained. In this study, we demonstrate that, in addition to producing H_2O_2 and ˙OH, O_2–˙can directly participate in the degradation of *p*-nitrophenol (PNP). EPR analysis and probe tests showed that $O_2^{\bullet-}$ was largely produced in the first 15 min of the reaction, during which PNP was rapidly degraded. Masking experiments indicated that O_2˙–, rather than O˙H, was the main ROS for the direct degradation of PNP. GC–MS and LC-MS– confirmed that O_2˙– reduced PNP to p-aminophenol. The PNP degradation pathway was proposed accordingly. Another two monocyclic aromatics with different functional groups were also investigated to further confirm the impact of O_2˙– on contaminant degradation. It was found that the degree of O_2˙– participation during direct degradation mainly depends on the molecular structures of the contaminants. In addition, STPP always maintains the ability of promoting Fe^{2+} to activate O_2 after adding Fe^{2+} four times in the system. The aforementioned results indicate that STPP can be reused in the reaction system.

1. Introduction

p-Nitrophenol (PNP) is one of the most important derivatives of phenol. It can seriously damage the kidneys, liver, and central nervous system, even at a low concentrations [1–3]. The physicochemical properties of PNP are shown in Table S1 [4–6]. The benzene ring of PNP contains hydroxyl and nitro groups. The hydroxyl group can be easily oxidized to quinolyl, while the nitro group tends to be reduced to an amino group [7]. Based on its high toxicity and low biodegradability, an advanced oxidation process (AOP) is considered a feasible approach to the treatment of PNP.

It was known that photogenerated electrons on the surface of semiconductors could activate molecular oxygen in photocatalytic process [8–11]. In addition, more and more scholars have found that Fe^{2+} can also activate O_2 to produce ˙OH and other reactive oxygen species (ROS) for contaminant oxidation [12–14]. The mechanisms for ROS production in Fe^{2+} activated O_2 are divided into two categories [15–18]: (1) One-electron transfer; in this case, Fe^{2+} activates O_2 to generate superoxide radicals (O_2˙–) (via reaction 1), then H_2O_2 and ˙OH are successively produced through reactions 2 and 4; and (2) two-electron transfer; In this case, Fe^{2+} activates O_2 to directly to generate H_2O_2 (via reaction 3). However, the yield of ROS in this Fe^{2+}/O_2 system is too low for application in environmental pollutant control and remediation. Recently, several researchers [19–21] have pointed out that polyphosphates, a group of relatively safe and low-cost inorganic chelators, dramatically promote the production of ROS by reducing the Fe^{2+}/Fe^{3+} electrode potential and inhibiting iron precipitation. They confirmed that ˙OH and $O_2^{-\cdot}$ were the main ROS in this system. The generation of ˙OH was dominated by the one-electron activation of O_2 ($O_2 \rightarrow O_2^{\cdot-} \rightarrow H_2O_2 \rightarrow O^{\cdot}H$). Wang et al. proved the crucial role of ˙OH during the degradation of sodium pentachlorophenol (NaPCP) [22]. When ˙OH is trapped by *tert*-butyl alcohol (TBA), the degradation of NaPCP was almost completely inhibited. Several other studies [17,23] have also demonstrated that ˙OH is the dominant ROS responsible for contaminant degradation. However, limited information is available on the potential of O_2˙– to transform different organic contaminants. O_2˙– has one unpaired electron and is the product of the one-electron reduction of dioxygen. A second reduction of O_2˙– requires the energetically disfavored compression of two full negative charges on a diatomic molecule. As a result, O_2˙– is generally a better reducing agent than oxidizing agent ($E_0(O_2/O_2^{\cdot-}) = -0.33$ V_{NHE} [24]. Watts et al. also demonstrated that O_2˙–, generated via a modified Fenton reaction, can effectively degrade perhalogenated alkanes and compounds with a high degree of nitro-substitution that are difficult to degrade using ˙OH

* Corresponding author.
E-mail address: qincyu@jlu.edu.cn (C. Qin).

https://doi.org/10.1016/j.apcatb.2019.118030
Received 25 February 2019; Received in revised form 19 July 2019; Accepted 29 July 2019
Available online 02 August 2019
0926-3373/

[25,26]. As a nucleophile, $O_2^{\cdot}-$ has the potential ability to reduce electron-deficient compounds bearing nitro and chlorine groups [27]. Therefore, in addition to the recognized transformation to H_2O_2 and $^{\cdot}OH$, it is important to investigate the other specific roles that $O_2^{\cdot}-$ can play during the degradation of organic contaminants in the Fe^{2+}/polyphosphate/O_2 system in depth. Although some researchers [22,28] have proposed that $O_2^{\cdot}-$ may participate in the reductive dechlorination of chlorinated aromatics in the Fe^{2+}/O_2 system, further information is still required to confirm and evaluate this hypothesis.

$$Fe^{2+} + O_2 \rightarrow Fe^{3+} + O_2^{\cdot}- \quad (1)$$

$$Fe^{2+} + O_2^{\cdot}- + 2H_2O \rightarrow Fe^{3+} + H_2O_2 + 2OH- \quad (2)$$

$$2Fe^{2+} + O_2 + 2H_2O \rightarrow 2Fe^{3+} + H_2O_2 + 2OH- \quad (3)$$

$$Fe^{2+} + H_2O_2 \rightarrow Fe^{3+} + {}^{\cdot}OH + OH- \quad (4)$$

In this study, sodium tripolyphosphate (STPP), one of the commonly used polyphosphates, was selected to improve the yield of ROS in the Fe^{2+}/O_2 system and PNP was used as the target contaminant. We investigated the degradation of PNP in the Fe^{2+}/STPP/O_2 system as a function of pH and the molar ratio of STPP to Fe^{2+}. ROS generation was systematically studied using scavenging and probe tests for free radicals, as well as electron paramagnetic resonance (EPR) spectroscopy, to clarify the mechanism of PNP degradation. By analyzing the intermediate products via gas chromatography–mass spectrometry (GC–MS) and liquid chromatography–mass spectrometry (LC–MS), we confirmed the role of $O_2^{\cdot}-$ during the degradation of PNP and proposed its degradation pathway. To further understand the effect of $O_2^{\bullet-}$ on contaminant degradation in the Fe^{2+}/STPP/O_2 system, two other monocyclic aromatic compounds bearing different substituents were investigated for comparison.

2. Materials and methods

2.1. Materials

Chemicals and materials used in this study are presented in Text S1

2.2. Experimental procedure

All experiments for PNP degradation were conducted in 250 mL glass bottles. A PNP stock solution was prepared by dissolving solid powdered PNP in deionized water with gentle stirring and then diluted to the desired concentration of 20 mg/L. Then, a certain amount of the STPP was dissolved in PNP solution. The solution pH was adjusted to 7.0 ± 0.1 (except for the experiments on the effect of pH on the degradation) using 1 mol/L HCl and NaOH solutions. Ferrous chloride was then added to initiate the degradation reaction with bubbling air at a flow rate of 150 mL/min. An air pump (ACO-001) from Guangdong Risheng Group Co., Ltd. (China) was used as the bubbling device. The initial concentration of ferrous ion was 25 mmol/L. The samples (1 mL) were withdrawn at scheduled time intervals, and ethanol was added to quench the reaction prior to the analysis of PNP. To identify the ROS generated during the reaction, probe tests were conducted in accordance with the PNP degradation procedure, except that PNP was replaced by salicylic acid (•OH probe) or NBT (Nitroblue tetrazolium chloride,$O_2^{\cdot -}$ probe). In addition, to evaluate the contributions of different ROS to the PNP degradation, TBA ($^{\cdot}OH$ scavenger), catalase (H_2O_2 scavenger) and 1,4-benzoquinone ($O_2^{\cdot -}$ scavenger) were used in the experiments to observe the PNP degradation changes. Four initial pH values (3.0, 5.0, 7.0 and 9.0) were chosen to observe the effect of pH on the PNP degradation. Different STPP concentrations (25, 50, 75, and 100 mmol/L) were also chosen to study the effect of STPP on the degradation. In other experiments, the initial STPP concentration was set to 50 mmol/L. All experiments were conducted in triplicate, and the analysis showed that the relative errors were lower than ± 5%.

2.3. Analysis

The concentrations of PNP, hydroquinone(HQ), p-hydroxy benzoic acid (p-HBA) and tetrabromobisphenol A were measured using high-performance liquid chromatograph (HPLC, Agilent 1100) with a C18 reversed-phase column, a UV detector and a fluorescence detector (FLD) (Text S2). Gas chromatography/mass spectrometry (GC/MS, Agilent 6890/5973) and liquid chromatography–mass spectrometry (LC–MS, Thermo TSQ) were used for the identification of the intermediate products in PNP degradation. The methods are explained in Text S3. A TOC analyzer (TOC-L, Shimadzu, Japan) was used to evaluate the mineralization of PNP. The active free radical was measured using electron paramagnetic resonance (EPR), and the trapping agent was 5,5-dimethyl-1-pyrroline N-oxide (DMPO). $^{\cdot}OH$ was determined in the aqueous phase. $O_2^{\cdot -}$ was determined in methanol solution. A spectrophotometer (Evolution, Thermo, America) was used to measure the following indicators during the experiment: (1) A modified 1,10-phenanthroline method was used to determine the concentration of ferrous ions. When the total iron concentration was measured, hydroxylamine hydrochloride was utilized as the reductant [29]; (2) the diformazan produced by the reaction of NBT with $O_2^{\cdot -}$ was measured at the wavelength of 560 nm and was used to qualitatively analyze the $O_2^{\cdot -}$content in the solution [30]; (3) the product of the reaction of salicylic acid with $^{\cdot}OH$ was determined at a wavelength of 510 nm by the sodium nitrite/sodium tungstate colorimetric method to qualitatively analyze the $^{\cdot}OH$ content in the solution [31]; and (4) the H_2O_2 content in the solution was measured at a wavelength of 340 nm using the ammonium molybdate chromogenic method [32]. The solution pH/ORP was analyzed using a pH/ORP meter from Shanghai San-Xin Instrumentation, Inc. (SX721, China). The solution dissolved oxygen was analyzed using a HACH (sensION + DO6, America) DO meter.

3. Results and discussion

3.1. Degradation of PNP using different systems

PNP degradation in the presence of different components is shown in Fig. 1a. In the Fe^{2+}/O_2/STPP system, PNP was degraded by > 80% in 40 min. In the other three reaction groups, the PNP concentration did not obviously change in > 60 min. From the results obtained for the Fe^{2+}/N_2/STPP system, we know that the volatilization loss of PNP caused by aeration was negligible. The results of the O_2/STPP system indicate that O_2 could not directly oxidize PNP. In the Fe^{2+}/O_2 system, Fe^{2+} alone was not effective toward activating O_2 to degrade PNP. Therefore, PNP degradation required the coexistence of Fe^{2+}, O_2, and STPP. Fig. 1b shows the variation in the concentration of Fe(II) and Fe (III) during the degradation of PNP. After the experiment began, the Fe^{2+} concentration quickly decreased and this trend was consistent with that of the degradation of PNP. This result confirmed that O_2 activation was closely related to the electron donation from Fe^{2+}. At the same time, the Fe^{3+} concentration increased correspondingly. The total iron content in the solution during the reaction was basically unchanged. This finding was attributed to the chelation of both Fe^{2+} and Fe^{3+} with the STPP ligand [23]. The Fe(II)–STPP complex effectively activates O_2 to produce ROS for PNP degradation, while the Fe (III)–STPP complex prevents the formation of iron precipitate, which is a common limitation in Fe-related AOPs. Fig. 1c shows the variation in the concentration of dissolved oxygen (DO) in the Fe^{2+}/O_2/STPP system. It was observed that the concentration of DO decreased sharply once the reaction began, further indicating that O_2 was rapidly activated by Fe^{2+} in the presence of STPP. Even though aeration was continuously operated, the supply of O_2 was still smaller than its consumption during the initial stage of the experiment. Furthermore, ORP accordingly declined to its lowest value of −169 mV (Fig. 1d). This low ORP value implies that the production of reductive species was highly likely. $O_2^{\cdot}-$ produced via the one-electron activation of O_2 was

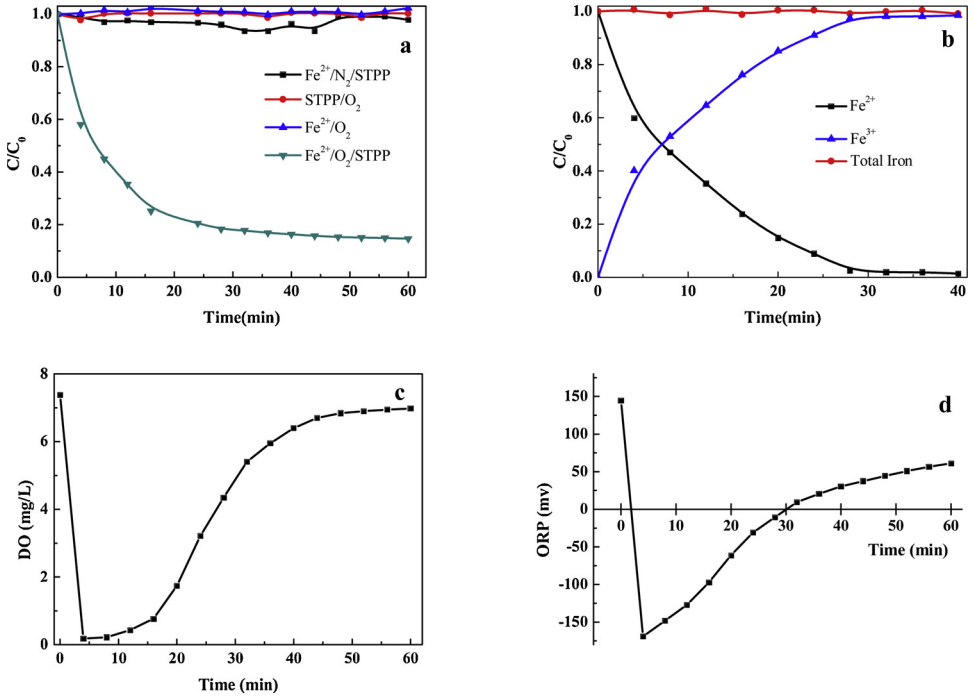

Fig. 1. (a) Degradation of PNP by the Fe^{2+}/O_2/STPP system and three control experiments. (b) Concentrations of the dissolved iron as a function of time in Fe^{2+}/O_2/STPP systems. The dissolved oxygen (c) and ORP(d) variations during the degradation of PNP in the Fe^{2+}/O_2/STPP system. The initial concentrations of PNP, Fe^{2+} and STPP were 20 mg/L, 25 mM, 50 mM, respectively. Initial pH was 7.0.

presumed to be the main substance in the reaction system, which leads to the decrease in the ORP value. This hypothesis will be analyzed in-depth below.

3.2. Effect of the initial pH

Experiments were performed at initial pH values of 3, 5, 7, and 9 (Fig. 2). As shown in Fig. 2b, the PNP degradation process was found to obey pseudo-first-order kinetics. The k_{obs} values were 0.021, 0.048, and 0.076 min^{-1} at pH 3, 5, and 7, respectively. This was attributed to the decrease in O_2 activation by the Fe^{2+}/STPP complexes, which results due to ligand protonation at low pH [22]. Specifically, under low pH conditions, the negatively charged $P_3O_{10}^{5-}$ ions reacts with a large amount of H^+ to generate $H_5P_3O_{10}$, which loses its complexing ability with Fe^{2+} and further reduces the degradation rate of PNP. Upon further increasing the pH to 9.0, the k_{obs} value decreased to 0.026 min^{-1}. This result was observed because the alkaline conditions not only inhibit the reaction of Fe^{2+} with O_2 to generate ROS, but also weaken the oxidation ability of ˙OH. Therefore, the optimal pH conditions for the reaction system was neutral, which is favorable for its practical application.

3.3. Effect of the molar ratio of Fe2+ to STPP

We kept the amount of Fe^{2+} in this system unchanged and set the Fe^{2+}/STPP molar ratio to 1:1, 1:2, 1:3,1:4 and 1:5, respectively. As shown in Fig. 3, the PNP degradation processes were found to obey pseudo-first-order kinetics at different Fe^{2+}/STPP molar ratios. In addition, the kobs has a linear relationship with the molar ratio of Fe^{2+}/STPP, indicating that the degradation rate of PNP was determined by the concentration of STPP in the system. The degradation rate of PNP increased upon increasing the STPP concentration, but the final removal values were almost identical. Therefore, considering the reaction rate and STPP dosage, we chose Fe^{2+}/STPP = 1:2 for the subsequent experiments.

3.4. Reactive oxygen species generation and degradation mechanism

According to previous research, the ROS produced in the Fe^{2+}/O_2 system are dominated by ˙OH and $O_2^{\bullet-}$ [14–16]. To confirm the type of ROS produced in this system, we utilized EPR spectroscopy and DMPO spin-trapping adducts to perform the analysis, and the results are shown in Fig. 4. Four characteristic peaks of a 1:2:2:1 quartet pattern (aN = aH = 14.9 G) were detected (Fig. 4a), indicating the generation of ˙OH [33,34]. From Fig. 4b, a 1:1:1:1 quadruple signal characteristic of the DMPO-$O_2^{\bullet-}$ spin adduct was observed, demonstrating the

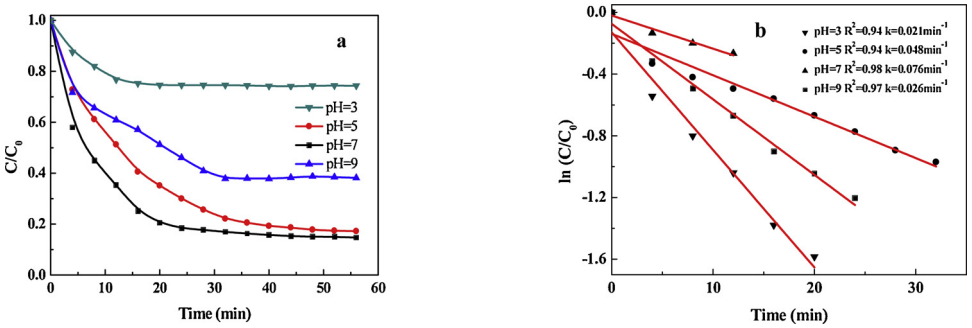

Fig. 2. The PNP degradation curve and plots of ln(C/C0) versus time obtained at different initial pH values. The initial concentrations of PNP, Fe^{2+} and STPP were 20 mg/L, 25 mM, 50 mM, respectively.

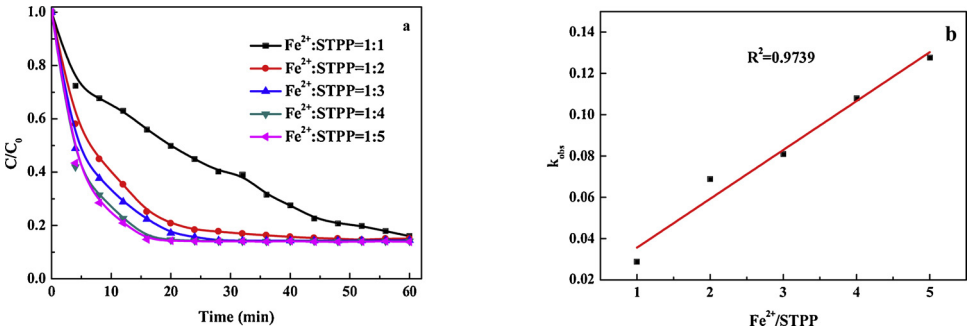

Fig. 3. (a) The PNP degradation curve obtained for the Fe^{2+}/O_2/STPP system at different Fe^{2+}/STPP molar ratios. (b) The correlation between the different Fe^{2+}/STPP molar ratios and k_{obs}. The initial concentrations of PNP, Fe^{2+} and STPP were 20 mg/L, 25 mM, and 50 mM, respectively. The initial pH values were 7.0.

presence of $O_2^{\cdot}-$ [35]. To further confirm the content of ROS in the system, we designed two groups of probe experiments. It is known that NBT can be used to detect $O_2^{\bullet-}$ because it does not react with other active oxygen species. NBT can react with $O_2^{\cdot}-$ to form diformazan, which has a characteristic absorption wavelength at 530 nm. Fig. 5a shows that $O_2^{\cdot}-$ was produced in large quantities at the beginning of the reaction and reached a maximum concentration at 5 min. For $^{\cdot}OH$, we used salicylic acid as the molecular probe. The reaction of salicylic acid with $^{\cdot}OH$ produces 2,5-dihydroxybenzoic acid (2,5-DHBA) and 2,3-dihydroxybenzoic acid (2,3-DHBA). These products were detected by spectrophotometry at 510 nm using sodium nitrite and sodium tungstate as the chromogenic agents. Fig. 5b shows that the amount of $^{\cdot}OH$ increased continuously after the experiment began and reached a maximum value at 28 min. Combining the results presented in these two figures, we found that the generation of $O_2^{\cdot}-$ and $O^{\cdot}H$ showed a clear sequence. This finding indicates that $^{\cdot}OH$ may be formed mainly via the one-electron activation of oxygen ($O_2 \rightarrow O_2^{\cdot}- \rightarrow H_2O_2 \rightarrow O^{\cdot}H$). The results of this study are in agreement with those previously reported in the literature [15,20]. Unfortunately, we could not detect the presence of H_2O_2 using the potassium iodine reduction method. It is possible that the H_2O_2 generated is rapidly consumed via the Fenton reaction with Fe^{2+} in the system, resulting in concentration of H_2O_2 being lower than the detection limit.

We next used TBA, catalase, and 1,4-benzoquinone (PBQ) as the scavengers of $^{\cdot}OH$, H_2O_2, and $O_2^{\cdot}-$, respectively. The relative contribution of each ROS toward PNP degradation was assessed by the addition of an excess of each scavenger. As shown in Fig. 6, PNP was degraded by more than 80% in the control experiment (without the scavenger). In contrast, only 8.9% of PNP was degraded after PBQ was added to the system. This small amount of degradation was attributed to the $^{\cdot}OH$ produced via a two-electron transfer mechanism ($O_2 \rightarrow H_2O_2 \rightarrow {}^{\cdot}OH$) [15,18]. This result implies that $O_2^{\cdot}-$ plays a crucial role in this Fe^{2+}/O_2 advanced oxidation system. When TBA was added to the system, PNP was degraded by 76.1%. This result proves that $^{\cdot}OH$ (produced via both one and two-electron transfer mechanisms) was not the main ROS accounting for the degradation of this contaminant. Furthermore, the PNP degradation curve obtained in the presence of the $^{\cdot}OH$ scavenger (TBA) was almost identical to that with the H_2O_2 scavenger (catalase). This finding further demonstrates that $^{\cdot}OH$ produced by the reaction of H_2O_2 with Fe^{2+} plays a minor role in the degradation of PNP. Fig. S1 shows the TOC variation in the system with time. The TOC remained almost unchanged during the entire reaction process. Although > 80% of PNP was transformed, very little was mineralized. Therefore, we hypothesize that the $O_2^{\cdot}-$ produced via the one-electron activation of O_2 directly participates in the degradation of PNP.

3.5. PNP degradation pathway

GC–MS was used to determine the intermediate products to identify the role of $O_2^{\cdot}-$ in PNP degradation. The mass spectrometry results obtained for the transformation intermediates at different reaction times are displayed in Fig. S2a–f. Fig. S3 and S4 show the final degradation products of PNP in the presence of the $O_2^{\cdot}-$ (PBQ) and $O^{\cdot}H$ (TBA) scavengers, respectively. Six main chemicals were identified with molecular weights ranging from 45 to 250, and the results are shown in Table 1. It was observed that p-aminophenol (the representative reduction product of PNP), p-nitrocatechol (the representative oxidation product of PNP), hydroquinone, and p-benzoquinone were all detected at 4, 8, and 16 min. This result means that the reduction and oxidation of PNP were performed simultaneously at the start of the reaction. After 16 min, p-aminophenol was not detected. p-Aminophenol was probably oxidized by $^{\cdot}OH$ to form hydroquinone [36]. This result indicates that $O_2^{\cdot}-$ plays the role of both reductant and oxidant. On one hand, $O_2^{\bullet-}$ reduces PNP to p-aminophenol and on the other hand, it oxidizes Fe^{2+} to form H_2O_2, which is further transformed into $^{\cdot}OH$. $O^{\cdot}H$ oxidizes p-aminophenol more easily when compared to PNP because of its higher electron cloud density. Simultaneously, hydroquinone, benzoquinone, and butanoic acid ethyl ester were detected in this system. The LC–MS results show that small molecular weight acids such as formic acid and acetic acid were detected in the system. Based on these intermediates, we can easily deduce the main PNP degradation pathway via the one-electron activation of O_2. To determine the PNP degradation pathway via the two-electron transfer mechanism, we monitored the final degradation products of PNP formed in the presence of the $O_2^{\cdot -}$ scavenger (PBQ). Hydroquinone and benzoquinone were still present in

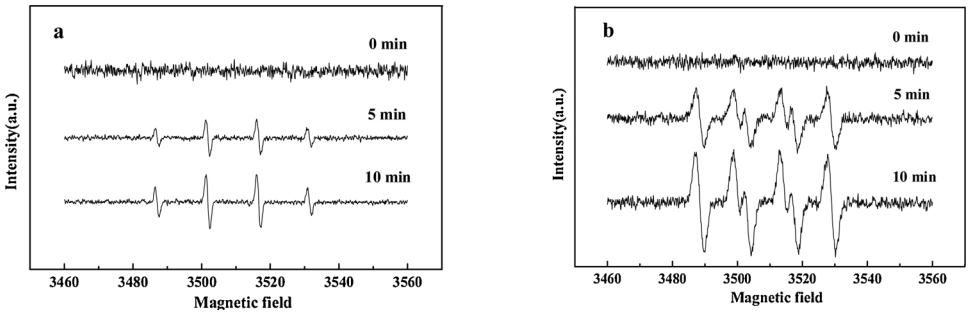

Fig. 4. DMPO spin-trapping EPR spectra recorded for $^{\cdot}OH$ (a) and $O_2^{\cdot}-$ (b) for the Fe^{2+}/O_2/STPP system. The concentration of DMPO was 25 mmol/L. $^{\cdot}OH$ was determined in the aqueous phase. $O_2^{\cdot}-$ was determined in a methanolic solution.

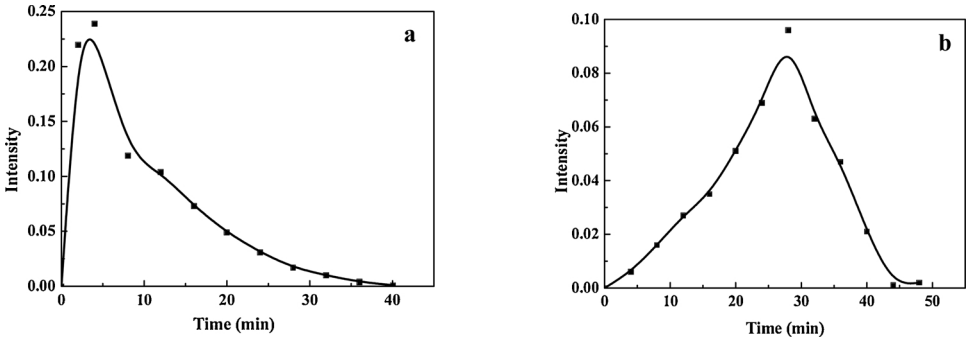

Fig. 5. (a) Detection of $O_2^{\cdot}-$ generated in the Fe^{2+}/O_2/STPP systems by spectrophotometry at 530 nm; (b) Detection of $^{\cdot}OH$ generated in the Fe^{2+}/O_2/STPP systems by spectrophotometry at 510 nm. The initial concentrations of PNP, Fe^{2+} and STPP were 20 mg/L, 25 mM, 50 mM, respectively. Initial pH values were 7.0.

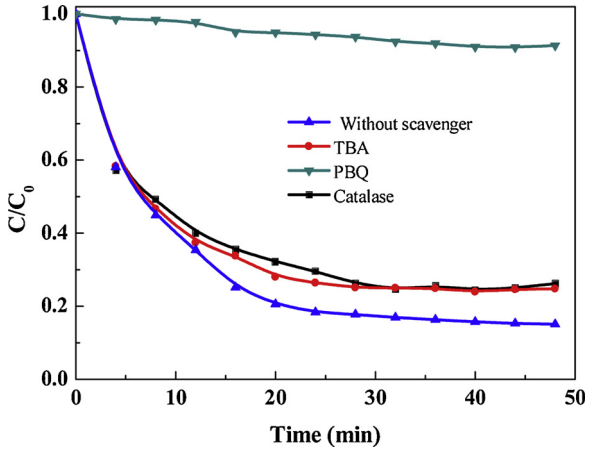

Fig. 6. Effect of scavengers on the degradation of PNP in the Fe^{2+}/O_2/STPP systems. The initial concentrations of PNP, Fe^{2+} and STPP were 20 mg/L, 25 mM, and 50 mM, respectively. The initial pH values were 7.0.

the system (Fig. S3). This result proves that PNP was first oxidized to *p-nitrocatechol*and *hydroquinone*. these products were further oxidized to benzoquinone [37,38]. However, no benzene ring-opening products were observed, which means that $^{\cdot}OH$ (only produced via a two-electron transfer mechanism) was not able to achieve the ring cleavage effect only because of it being formed in relatively low quantities. As for the final degradation products of PNP formed in the presence of the $^{\cdot}OH$ scavenger (TBA), only a large peak corresponding to *p*-aminophenol was observed, further proving the direct reaction of $O_2^{\cdot}-$ and PNP. Considering these experimental results and taking into account the information reported in the literature [39,40], the reaction pathway for the degradation of PNP was proposed and is shown in Fig. 7. It should be noted that although we tried to quantitatively test the main intermediate products (p-aminophenol and p-nitrocatechol) formed during the reaction, their concentrations were too low and too variable to be analyzed. This outcome may be due to their quick consumption by $^{\cdot}OH$, leading to much smaller concentrations and the instability of these intermediates.

3.6. Effect of the molecular structures of pollutants on their transformation by O2˙–

$^{\cdot}O2-$ is a weakly reducible nucleophilic free radical that can easily attack the low electron cloud density region of molecules [25]. Based on the above results, the reduction of PNP by $O_2^{\cdot}-$ seems to be easy because the nitro group located on the benzene ring is a strong electron-withdrawing group. Therefore, $O_2^{\cdot}-$ is the main ROS for the direct degradation of PNP. However, Wang et al. [22] used a Fe^{2+}/tetrapolyphosphate/O_2 system to degrade NaPCP. Their results showed that although $O_2^{\cdot}-$ participated in the NaPCP degradation process, $^{\cdot}OH$ played the main role. The main origin of these inconsistent conclusions probably lies in the different molecular structures of the contaminants. To verify our hypothesis, phenolic compounds HQ and p-HBA were selected as target pollutants to test their degradation performance in the Fe^{2+}/O_2/STPP system. It is well-known that the carboxyl group is a weak electron-withdrawing group and hydroxyl is an electron-donating group. Therefore, the electron cloud density of the benzene ring is

Table 1
Determination of the intermediates formed at different reaction times using GC–MS.

Symbol	Compound	Structural formula	Sampling time (min)					
			4	8	16	24	32	40
A_1	*p*-Nitrophenol	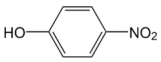	√	√	√	√	√	√
A_2	*p*-Aminophenol	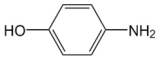	√	√	√			
A_3	*p*-Nitrocatechol	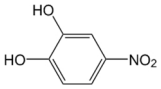	√	√	√	√		
A_4	Hydroquinone	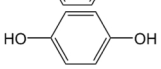	√	√	√	√	√	√
A_5	Benzoquinone		√	√	√	√	√	√
A_6	Butanoic acid ethyl ester	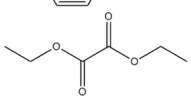					√	√

"√"indicates that the substance was detected.

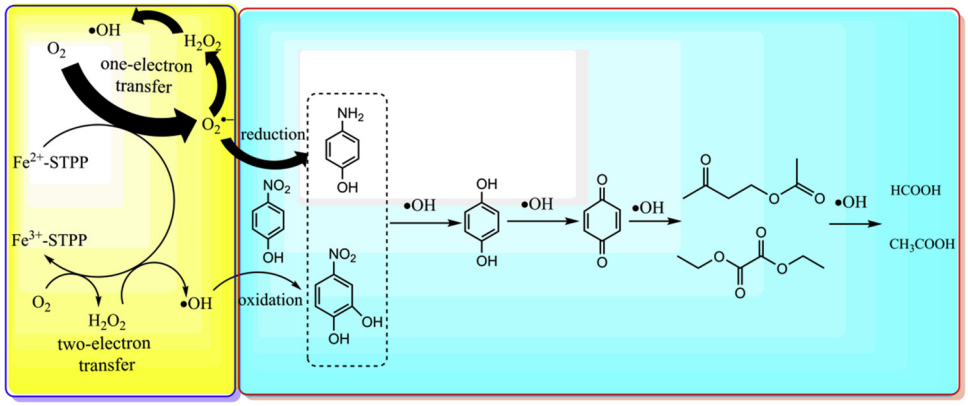

Fig. 7. A possible degradation pathway for PNP in the Fe^{2+}/O_2/STPP system.

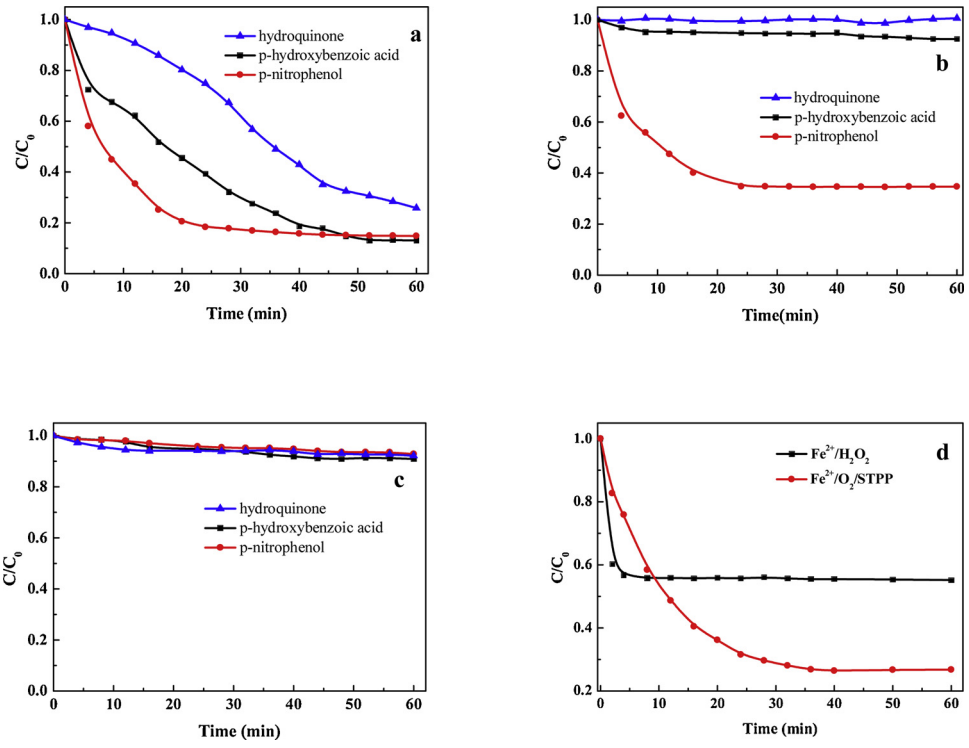

Fig. 8. (a) Degradation of PNP, HQ and p-HBA by the Fe^{2+}/O_2/STPP system and the effect of the radical scavengers on its degradation. The radical scavengers in (b) and (c) were TBA and PBQ, respectively. The initial concentrations of PNP, HQ and p-HBA were 20 mg/L. The initial concentrations of Fe^{2+} and STPP were 25 mM, and 50 mM, respectively. The initial pH values were 7.0.(d) The degradation curves obtained for tetrabromobisphenol A using Fe^{2+}/H_2O_2 and Fe^{2+}/O_2/STPP systems. The initial concentration of tetrabromobisphenol A was 5 mg/L.

ranked as follows: PNP < p-HBA < HQ. A comparison of the degradation performance observed for the three contaminants is shown in Fig. 8a. All three contaminants were effectively degraded, but the degradation patterns were different. As discussed above, PNP was quickly removed during the first 15 min due to reduction by $O_2^{\bullet-}$. In contrast, HQ had the lowest degradation rate during the initial period of the reaction. This was attributed to HQ being hardly transformed by $O_2^{\bullet-}$. Only O˙H that was largely generated at ˜30 min (Fig. 5b) leads to the rapid removal of HQ at a relatively later time. The degradation curve obtained for p-HBA was between the other two curves, which is in accordance with the electron cloud density of these three phenolic compounds. Fig. 8b shows the curve obtained for the degradation of the three contaminants in the presence of TBA (˙OH scavenger). As we suggested, no HQ was degraded in the absence of •OH. The small amount of p-HBA degradation observed was mainly due to its reduction by $O_2^{\bullet-}$. Therefore, the order of contaminant decomposition by $O_2^{\bullet-}$ was HQ < p-HBA < PNP, which is exactly the opposite order observed for the electron cloud density. This finding fully demonstrates that the molecular structures of the pollutants determine the role of $O_2^{\bullet-}$ in their degradation. The stronger the electron withdrawing ability, the greater the contribution from $O_2^{\bullet-}$ to the degradation of the pollutant. As shown in Fig. 8c, when PBQ ($O_2^{\bullet-}$ scavenger) was added to the system, little difference was observed in the degradation of the three pollutants. This was attributed to ˙OH, unlike $O_2^{\bullet-}$ and other radical species, is capable of reacting non-selectively with different organic contaminants. However, because of the small amount of ˙OH produced via the two-electron transfer pathway, < 10% of the contaminants are degraded.

In order to further prove the role of $O_2^{\bullet-}$ in Fe^{2+}/O_2/STPP system, tetrabromobisphenol A (a Poly Brominated Diphenyl Ether) was selected as the target pollutant for degradation process. Tetrabromobisphenol A ($C_{15}H_{12}Br_4O_2$) is one of brominated flame retardants. Generally, it is very resistant to oxidative degradation in the environment due to its strong electron-withdrawing ability resulting from their bromine substituents. Therefore, reductive debromination becomes a key step in degradation and mineralization of tetrabromobisphenol A. The degradation of tetrabromobisphenol A in the Fe^{2+}/O_2/STPP system and the conventional Fenton system (Fe^{2+}/H_2O_2) is shown in Fig. 8d. Using benzoic acid as a probe, we determined that the •OH produced by the two systems is almost identical.

(Fig. S5). The results shown that although tetrabromobisphenol A was rapidly degraded within 4 min of the reaction in Fe^{2+}/H_2O_2 system, its final degradation rate was only 40%. In the Fe^{2+}/O_2/STPP system, the degradation rate of tetrabromobisphenol A reached 40% after 10 min of reaction, and the final degradation rate was 74%, which was much higher than that in Fe^{2+}/H_2O_2 system. Fig. S6 illustrates the change of TOC in both systems. We found that the TOC in Fe^{2+}/H_2O_2 system decreased rapidly to 83% in the first ten minutes and then remained basically unchanged. There is no doubt that the decrease of TOC is caused by the contaminant mineralization by ˙OH. On the contrary, the TOC in Fe^{2+}/O_2/STPP system has hardly changed in the first 20 min, nevertheless, the target contaminant (tetrabromobisphenol A) concentration has been reduced by more than 60% during this time. As shown in Fig. 5, the content of ˙OH was very low in the first 20 min. So it's easy to conclude that most of the contaminants were degraded by $O_2^{\cdot}-$ in this period. After 20 min of reaction, the TOC decreased rapidly because large amount of ˙OH produced in the system can easily degrade reduction intermediate products. Therefore, the final tetrabromobisphenol A degradation and TOC removal were higher in this reduction-oxidation coupling system (Fe^{2+}/O_2/STPP).

3.7. The role of STPP in the reaction system

Cyclic voltammograms of Fe^{2+} and Fe^{2+}-STPP solutions are shown in Fig. 9a. For the Fe^{2+} solution, a peak is observed at ~0.8 V during the positive scan. After STPP was added, the peak potential dropped to ~0.2 V. This indicates that STPP can effectively decrease the redox potential of Fe^{3+}/Fe^{2+}. Then, we determined the STPP content in the system before and after the reaction using ion chromatography. As shown in Fig. 9b, the results showed that STPP always maintains its initial concentration during the reaction. In order to determine the reusability of STPP, Fe^{2+} was repeatedly added to the Fe^{2+}/O_2/STPP system to degrade 1 g/L PNP (The solution pH was adjusted to 7.0 ± 0.1 before each addition of Fe^{2+}). As displayed in Fig. 9c, PNP in the system could still be effectively degraded after repeated addition of Fe^{2+} four times. The above experimental results indicate that that STPP can be reused in the system.

4. Conclusions

In this study, a Fe^{2+}/STPP/O_2 system was proven to be dramatically efficient in the PNP degradation process. Surprisingly, ˙OH, which is generally considered the main ROS for contaminant decomposition, makes only a slight contribution to the direct degradation of PNP. In contrast, $O_2^{\cdot}-$ generated via the one-electron activation of O_2 plays a crucial role in the degradation of PNP. On the one hand, $O_2^{\cdot}-$ reduces most of the PNP to *p*-aminophenol acting as a reductant, but on the other hand, it oxidizes Fe^{2+} to form ˙OH, which is the main ROS for the oxidation of p-aminophenol and other intermediates. This finding shows that $O_2^{\cdot}-$ plays the role of both reductant and oxidant in this system. In the Fe^{3+}-H_2O_2 modified-Fenton system, Watts and other researchers also confirmed the dual effect of $O_2^{\cdot}-$. However, this system required much higher H_2O_2 concentrations and lower pH to maintain the reduction ability of $O_2^{\cdot}-$ toward the oxidized compounds. When compared to the complicated Fe^{3+}-H_2O_2 modified-Fenton system, our novel Fe^{2+}/STPP/O_2 system is greener and more convenient. The dual effect of $O_2^{\cdot}-$ can be achieved by the activation of oxygen in a neutral environment [22,37]. This new finding may be important because almost all categories of organic contaminants can be efficiently degraded in this reduction-oxidation coupling system. Normal organic compounds can be easily oxidized by ˙OH, while for refractory compounds (e.g., polybrominated diphenyl ethers, such as tetrabromobisphenol A) that are strongly resistant to oxidation due to the powerful electron-withdrawing ability of their halogen substituents may be sequentially dehalogenated and ring-opened in this simple ferrous–polyphosphate/O_2 system. Therefore, this study is helpful for expanding the practical applications of this green and efficient advanced oxidation technology.

Conflict of interest

The authors declare that they have no known competing financial interests or personal relationships that could have appeared to influence the work reported in this paper.

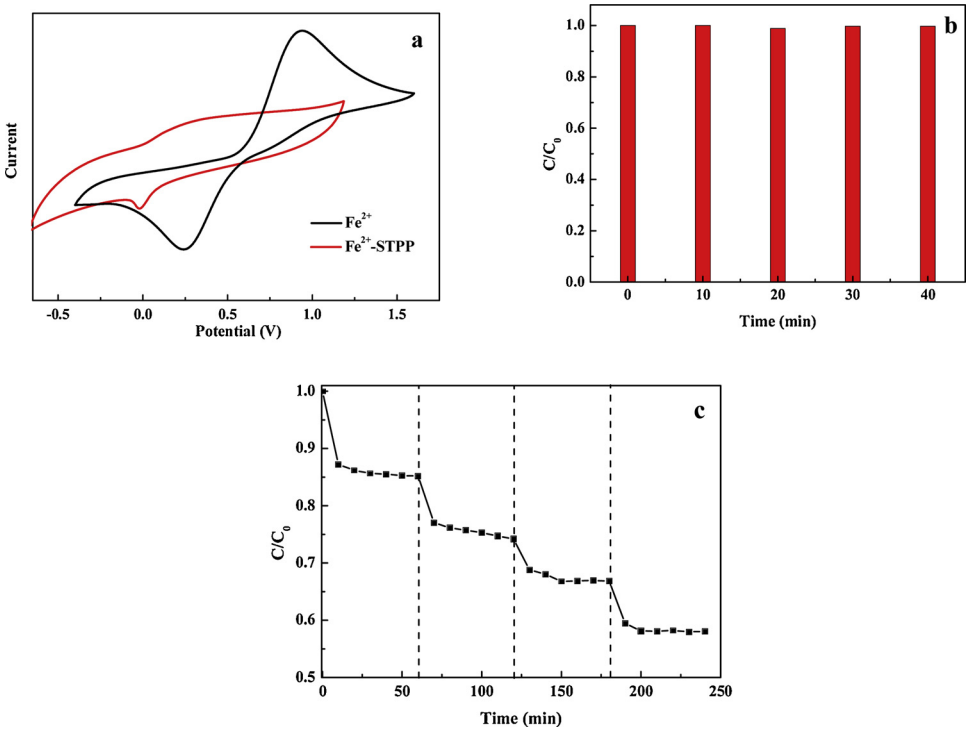

Fig. 9. (a) Cyclic voltammograms of Fe^{2+} and Fe^{2+}-STPP solutions.(b) The variation of STPP concentration during the reaction.(c) The degradation curve of PNP after adding Fe^{2+} four times in the system. The initial concentrations of PNP, and STPP were 1 g/L and 50 mM, respectively. The concentration of Fe^{2+} added each time is 25mM.

Acknowledgments

This work was financially supported by the National Natural Science Foundation of China (41572213), Key Project of National Natural Science Foundation of China (41530636), and the Fundamental Research Funds for the Central Universities of China.

Appendix A. Supplementary data

Supplementary material related to this article can be found, in the online version, at doi:https://doi.org/10.1016/j.apcatb.2019.118030.

References

[1] S. Yi, W.Q. Zhuang, B. Wu, S.T. Tay, J.H. Tay, Biodegradation of *p*-nitrophenol by aerobic granules in a sequencing batch reactor, Environ. Sci. Technol. 40 (2006) 2396–2401.
[2] J. Shen, X. Xu, X. Jiang, C. Hua, L. Zhang, X. Sun, J. Li, M. Yang, L. Wang, Coupling of a bioelectrochemical system for *p*-nitrophenol removal in an upflow anaerobic sludge blanket reactor, Water Res. 67 (2014) 11–18.
[3] Z. Ma, Z. Lin, X. Lu, S. Xing, Y. Wu, Y. Gao, Catalytic ozonation of *p*-nitrophenol over mesoporous Mn–Co–Fe oxide, Sep. Purif. Technol. 133 (2014) 357–364.
[4] G.H. Parsons, C.H. Rochester, C.E.C. Wood, Effect of 4-substitution on the thermodynamics of hydration of phenol and the phenoxide anion, J. Chem. Soc. B Phys. Org. (1971) 533–536.
[5] M. Riederer, Thermodynamic analysis of nonelectrolyte sorption in plant cuticles: the effects of concentration and temperature on sorption of 4-nitrophenol, Planta 169 (1986) 69–80.
[6] L.X. Yang, High efficient photocatalytic degradation of p-nitrophenol on a unique Cu_2O/TiO_2 p-n heterojunction network catalyst, Environ. Sci. Technol. 44 (2010) 7641–7646.
[7] M. Pandurangappa, T. Ramakrishnappa, R.G. Compton, Functionalization of glassy carbon spheres by ball milling of aryl diazonium salts, Carbon 47 (2009) 2186–2193.
[8] K. Seung-Hee, C. Wonyong, Oxidative degradation of organic compounds using zero-valent iron in the presence of natural organic matter serving as an electron shuttle, Environ. Sci. Technol. 43 (2009) 878–883.
[9] A.H. Mamaghani, F. Haghighat, C.S. Lee, Photocatalytic oxidation technology for indoor environment air purification: the state-of-the-art, Appl. Catal. B 203 (2017) 247–269.
[10] H. Huang, X.W. Li, J. Wang, D. Fan, P.K. Chu, T. Zhang, Y. Zhang, Anionic group self-doping as a promising strategy: band-gap engineering and multi-functional applications of high-performance CO_3^{2-} Doped $Bi_2O_2CO_3$, ACS Catal. 5 (2016) 150603114219008.
[11] H. Huang, S. Tu, C. Zeng, T. Zhang, A.H. Reshak, Y. Zhang, Macroscopic polarization enhancement promoting photo- and piezoelectric-induced charge separation and molecular oxygen activation, Angew. Chem. Int. Ed. 56 (2017).
[12] M. Tong, S. Yuan, S. Ma, M. Jin, D. Liu, D. Cheng, X. Liu, Y. Gan, Y. Wang, Production of abundant hydroxyl radicals from oxygenation of subsurface sediments, Environ. Sci. Technol. 50 (2016) 4890–4891.
[13] S.E. Page, G.W. Kling, M. Sander, K.H. Harrold, J.R. Logan, K. Mcneill, R.M. Cory, Dark formation of hydroxyl radical in Arctic soil and surface waters, Environ. Sci. Technol. 47 (2013) 12860–12867.
[14] M. Minella, L.E. De, V. Maurino, C. Minero, D. Vione, Dark production of hydroxyl radicals by aeration of anoxic lake water, Sci. Total Environ. 527–528 (2015) 322–327.
[15] C.R. Keenan, D.L. Sedlak, Factors affecting the yield of oxidants from the reaction of nanoparticulate zero-valent iron and oxygen, Environ. Sci. Technol. 42 (2008) 5377 author reply 5378.
[16] S.-Y. Pang, J. Jiang, J. Ma, Oxidation of sulfoxides and arsenic(III) in corrosion of nanoscale zero valent iron by oxygen: evidence against ferryl ions (Fe(IV)) as active intermediates in Fenton reaction, Environ. Sci. Technol. 45 (2011) 307–312.
[17] C.R. Keenan, C. Lee, D.L. Sedlak, Generation of oxidants from the reaction of nanoparticulate zero-valent iron and oxygen for the use in contaminant remediation, AGU Fall Meeting, (2007).
[18] C.R. Keenan, D.L. Sedlak, Ligand-enhanced reactive oxidant generation by nanoparticulate zero-valent iron and oxygen, Environ. Sci. Technol. 42 (2008) 6936.
[19] J.E. Biaglow, A.V. Kachur, The generation of hydroxyl radicals in the reaction of molecular oxygen with polyphosphate complexes of ferrous ion, Radiat. Res. 148 (1997) 181–187.
[20] L. Wang, M. Cao, Z. Ai, L. Zhang, Dramatically enhanced aerobic atrazine degradation with $Fe@Fe_2O_3$ core–shell nanowires by tetrapolyphosphate, Environ. Sci. Technol. 48 (2014) 3354–3362.
[21] J. Majeed, K.C. Barick, N.G. Shetake, B.N. Pandey, P. Hassan, A.K. Tyagi, Water-dispersible polyphosphate grafted Fe_3O_4 nanomagnets for cancer therapy, RSC Adv. 5 (2015) 86754–86762.
[22] L. Wang, F. Wang, P. Li, L. Zhang, Ferrous–tetrapolyphosphate complex induced dioxygen activation for toxic organic pollutants degradation, Sep. Purif. Technol. 120 (2013) 148–155.
[23] X. Hou, W. Shen, X. Huang, Z. Ai, L. Zhang, Ascorbic acid enhanced activation of oxygen by ferrous iron: a case of aerobic degradation of rhodamine B, J. Hazard. Mater. 308 (2016) 67–74.
[24] S. Ghosh, N.A. Kouamé, L. Ramos, S. Remita, A. Dazzi, A. Denisetbesseau, P. Beaunier, F. Goubard, P.H. Aubert, H. Remita, Conducting polymer nanostructures for photocatalysis under visible light, Nat. Mater. 14 (2015) 505.
[25] R.J. Watts, B.C. Bottenberg, T.F. Hess, M.D. Jensen, A.L. Teel, Role of reductants in the enhanced desorption and transformation of chloroaliphatic compounds by modified Fenton's reactions, Environ. Sci. Technol. 33 (1999) 3432–3437.
[26] B.A. Smith, A.L. Teel, R.J. Watts, Identification of the reactive oxygen species responsible for carbon tetrachloride degradation in modified Fenton's systems, Environ. Sci. Technol. 38 (2004) 5465–5469.
[27] Y. Li, J. Niu, L. Yin, W. Wang, Y. Bao, J. Chen, Y. Duan, Photocatalytic degradation kinetics and mechanism of pentachlorophenol based on Superoxide radicals, J. Environ. Sci. 23 (2011) 1911–1918.
[28] C.L. Cozza, A model for the prediction of biologically mediated reductive dechlorination pathways, Reduction (Chemistry) – Computer Simulation, (1990).
[29] J.D. Laat, Y.H. Dao, N.H.E. Najjar, C. Daou, Effect of some parameters on the rate of the catalysed decomposition of hydrogen peroxide by iron(III)-nitrilotriacetate in water, Water Res. 45 (2011) 5654–5664.
[30] T.V. Sirota, Standardization and regulation of the rate of the superoxide-generating reaction of adrenaline autoxidation used for evaluation of pro/antioxidant properties of various materials, Biochem. Mosc. Suppl. Ser. A Membr. Cell Biol. (Mosc) 11 (2017) 128–133.
[31] L. Milne, I. Stewart, D.H. Bremner, Comparison of hydroxyl radical formation in aqueous solutions at different ultrasound frequencies and powers using the salicylic acid dosimeter, Ultrason. Sonochem. 20 (2013) 984–989.
[32] C. Chen, Z. Gao, X. Qiu, S. Hu, Enhancement of the controlled-release properties of chitosan membranes by crosslinking with suberoyl chloride, Molecules 18 (2013) 7239.
[33] A. Fadda, A. Barberis, D. Sanna, Influence of pH, buffers and role of quinolinic acid, a novel iron chelating agent, in the determination of hydroxyl radical scavenging activity of plant extracts by Electron Paramagnetic Resonance (EPR), Food Chem. 240 (2017) 174.
[34] K. Fukuhara, T. Nakashima, M. Abe, T. Masuda, H. Hamada, H. Iwamoto, K. Fujitaka, N. Kohno, N. Hattori, Suplatast tosilate protects the lung against hyperoxic lung injury by scavenging hydroxyl radicals, Free Radic. Biol. Med. 106 (2017) 1.
[35] C.E. Diaz-Uribe, M.C. Daza, F. Martínez, E.A. Páez-Mozo, C.L.B. Guedes, E.D. Mauro, Visible light superoxide radical anion generation by tetra(4-carboxyphenyl)porphyrin/TiO_2: EPR characterization, J. Photochem. Photobiol. A: Chem. 215 (2010) 172–178.
[36] E. Moctezuma, E. Leyva, C.A. Aguilar, R.A. Luna, C. Montalvo, Photocatalytic degradation of paracetamol: intermediates and total reaction mechanism, J. Hazard. Mater. 243 (2012) 130–138.
[37] M. Zhou, L. Lei, An improved UV/Fe^{3+} process by combination with electrocatalysis for p-nitrophenol degradation, Chemosphere 63 (2006) 1032–1040.
[38] Y. Liu, D. Wang, B. Sun, X. Zhu, Aqueous 4-nitrophenol decomposition and hydrogen peroxide formation induced by contact glow discharge electrolysis, J. Hazard. Mater. 181 (2010) 1010–1015.
[39] D. Wan, W. Li, G. Wang, L. Lu, X. Wei, Degradation of *p*-Nitrophenol using magnetic Fe_0/Fe_3O_4/Coke composite as a heterogeneous Fenton-like catalyst, Sci. Total Environ. 574 (2017) 1326–1334.
[40] A.L. Teel, R.J. Watts, Degradation of carbon tetrachloride by modified Fenton's reagent, J. Hazard. Mater. 94 (2002) 179–189.